scientific reports

Check for updates

OPEN

Copper adorned magnetic nanoparticles as a heterogeneous catalyst for Sonogashira coupling reaction in aqueous media

Safoora Sheikh[1,2]✉, Mohammad Ali Nasseri[1]✉, Ali Allahresani[1] & Rajender S. Varma[3]

A nanomagnetic hydrophilic heterogeneous copper catalyst, termed γ-Fe_2O_3@PEG@PAMAM G_0-Cu, has been successfully prepared and characterized using FT–IR, XRD, FE-SEM, TEM, EDX, mapping, TGA/DTG, VSM and ICP analyses. The catalyst displayed excellent activity for the palladium-free Sonogashira cross coupling reaction of various aryl iodides and bromides with phenylacetylene derivatives in pure water. The presence of polyethylene glycol coupled with hydrophilic character of the Cu-catalyst adorned on γ-Fe_2O_3 MNPs provides the ready dispersion of the catalyst particles in water, leading to higher catalytic performance as well as facile catalyst recovery via simple magnetic decantation. The recovered catalyst was reused for at least six successive runs with little reduction in its catalytic activity and any noticeable changes in its structure. The use of water as a green solvent, without requiring any additive or organic solvent, as well as the exploitation of abundant and low-cost copper catalyst instead of expensive Pd catalyst along with the catalyst recovery and scalability, make this method favorable from environmental and economic points of view for the Sonogashira coupling reaction.

Green chemistry entails the design for eco-friendly methods that at its core consider health and safety in line with the environmental preservation and economic aspects[1,2]. The 12 principles of green chemistry comprise, among others, the optimal use of energy, reduce or eliminate hazardous processes, lessening waste while promoting the use of renewable resources[3]. So, considering the vital role of chemistry in human life, one of the main objectives is to eliminate environmental hazardous parameters in chemical reactions via greener processes[4]. The promotion of catalytic protocols in aqueous solvents—instead of toxic and dangerous solvents—or the deployment of heterogeneous/recoverable catalysts, to a large extent, are considered measures of environmental friendliness in the chemical reactions[5]. Among suitable platforms, magnetic nanoparticles have garnered attention due to their ease of preparation, high active surface area and easy surface modification as stabilizing surfaces for homogeneous catalysts[6–8]; magnetic nature of nanoparticles is a simple way to recycle these catalysts deploying an external magnet. This separation method does not require much time and energy compared to centrifugation and filtration methods thus preventing the catalyst from being wasted during the separation process while enhancing the purity of products and reducing costs. Among magnetic nanoparticles, γ-Fe_2O_3 is one of the most widely used metal oxides which are often utilized in the preparation of heterogeneous catalysts[9].

On the other hand, considering advantages of water as a green solvent, which is non-toxic, non-flammable, inexpensive and widely available, it can be a good alternative to toxic organic solvents[10]. Therefore, the design of efficient catalytic systems for organic synthesis in aqueous media is one of the sustainable means to adhere to the tenets of green chemistry[11–13]. However, often due to the insolubility or low solubility of the reaction materials in water, its use as a solvent has been limited and often necessitates the use additives such as surfactants, or auxiliary solvents for the enhancement of the reaction[14]. A desirable strategy that avoids the use of these additives is the deployment of hydrophilic catalysts that are well dispersed in the reaction medium. Various methods for the synthesis of hydrophilic catalysts have been proposed so far[15] including adorning solid catalysts encompassing

[1]Department of Chemistry, Faculty of Basic Sciences, University of Birjand, P. O. Box 97175-615, Birjand, Iran. [2]Institut Für Organische Chemie, Universität Regensburg, Universitätsstr. 31, 93053 Regensburg, Germany. [3]Regional Centre of Advanced Technologies and Materials, Czech Advanced Technology and Research Institute, Palacký University in Olomouc, ˇSlechtitelů 27, 783 71 Olomouc, Czech Republic. ✉email: sheikhsafoora90@gmail.com; Safoora.sheikh@chemi.uni-regensburg.de; manaseri@birjand.ac.ir

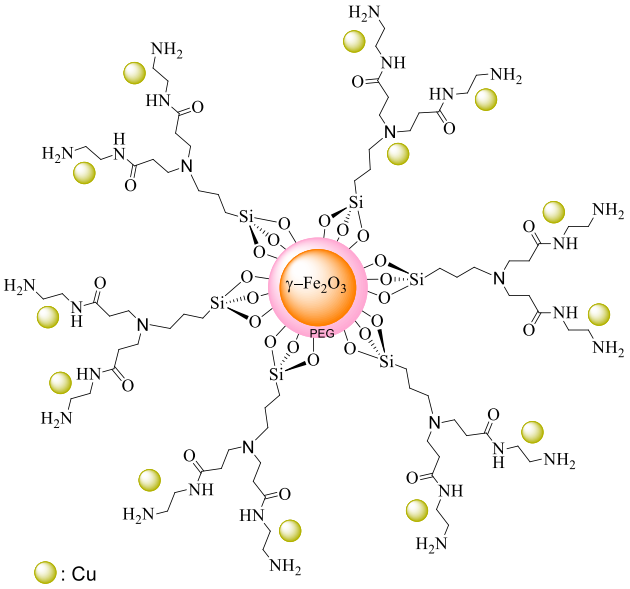

Figure 1. The proposed structure of γ-Fe_2O_3@PEG@PAMAM G_0-Cu.

magnetic core with hydrophilic compounds, which can be a powerful tool in the synthesis of water dispersible metal complexes[16].

Therefore, in view of the numerous favorable attributes of aforementioned magnetic nanoparticles (MNPs), modifying their surface to render them water dispersible is a key strategy; assorted hydrophilic materials such as cellulose, chitosan, polyethylene glycol have been explored earlier[17–20].

The formation of carbon–carbon bonds in cross-coupling reactions is considered as one of the most important organic chemistry reactions, which have been extremely practical and useful tools for the formation of complex molecules from simple molecules[21–24]. Asymmetric carbon–carbon coupling reactions are equally important and valuable in the synthesis of natural and medicinal compounds[25]. The most prominent and well-recognized transverse couplings are Heck, Negishi, Suzuki and Sonogashira reactions[26]. The importance and superiority of this group of reactions in organic chemistry is affirmed by the award of the Nobel Prize in Chemistry in 2010 to Professors Heck, Negishi and Suzuki[27] Sonogashira reaction was first reported by Sonogashira research group using Pd^0/Cu^I-catalyst, in 1975[28].

So far, various and powerful catalysts have been designed and synthesized to promote the Sonogashira cross-coupling reaction[29–31]. However, the copper complexes are often deployed to catalyze this reaction and most of these complexes are insoluble in water[32]. Therefore, the design of active copper catalysts usable in water as a green and abundant solvent, is still challenging[15].

Herein, as a part of our ongoing efforts to develop green and water dispersible catalysts, we describe the assembly of a copper-PAMAM dendrimer G_0 catalyst anchored on polyethylene glycol coated γ-Fe_2O_3, through the siloxy linker, γ-Fe_2O_3@PEG@PAMAM G_0-Cu (Fig. 1) and exemplified its performance and utility in the Sonogashira cross coupling as the target reaction, because diphenylacetylene derivatives are the precursors of drugs and biological substances and found in a wide variety of natural products and pharmaceutical agents (Fig. 2)[25].

Experimental section

Preparation of γ-Fe_2O_3@PEG@PAMAM-Cu MNPs. The various steps of catalyst preparation are depicted in Fig. 3. Initially, γ–Fe_2O_3 MNPs were synthesized via co-precipitation method as reported in the literature[33]. Subsequently, γ-Fe_2O_3@PEG MNPs were prepared using the previous described method[34].

To obtain γ-Fe_2O_3@PEG@APTES, γ-Fe_2O_3@PEG MNPs (1.0 g) was dispersed by sonication in dry toluene (30 mL) for 30 min. Then, (3-aminopropyl)triethoxysilane (APTES, 0.885 g, 0.83 mL, 4.0 mmol) was added dropwise to resulting dispersed solution of γ-Fe_2O_3@PEG MNPs, while the reaction was stirred under N_2, at 25 °C. Then, the temprature was raised to reflux conditions and heating continued for 24 h. After completion of the reaction, the solid product was separated from the solvent using an external magnet and washed twice with anhydrous toluene and diethyl ether and then dried under vacuum 50 °C overnight, to obtain γ-Fe_2O_3@PEG@APTES (1.12 g).

Subsequently, methyl acrylate (MAc, 7 mL, 6.6 g) was added dropwise to mixture of γ-Fe_2O_3@PEG@APTES (1.0 g) dispersed in ethanol (30 mL), while the reaction was stirred under N_2 atmosphere, at 25 °C. In the next step, the mixture was stirred and heated at 40 °C and the reaction continued for 24 h under N_2. After completion of the reaction, solid product was separated by an external magnet and washed with ethanol three times and followed by vacuum drying at 50 °C overnight, to acquire γ-Fe_2O_3@PEG@MAc (1.21 g).

Subsequently, the γ-Fe_2O_3@PEG@PAMAM G_0, was prepared by dispersion of 1 g of γ-Fe_2O_3@PEG@MAc in ethanol (40 mL) via sonication for 30 min, followed by addition of ethylenediamine (EDA, 0.1 mmol, 6.3 g) dissolved in ethanol (30 mL), while the reaction was being stirred under N_2, at 25 °C. Then, the temprature was

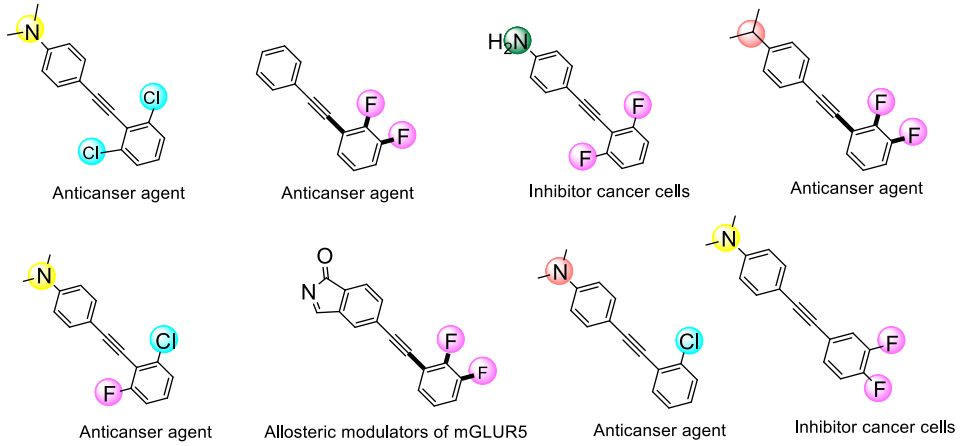

Figure 2. A few representative pharmacologically active compounds containing diphenylacetylene moieties.

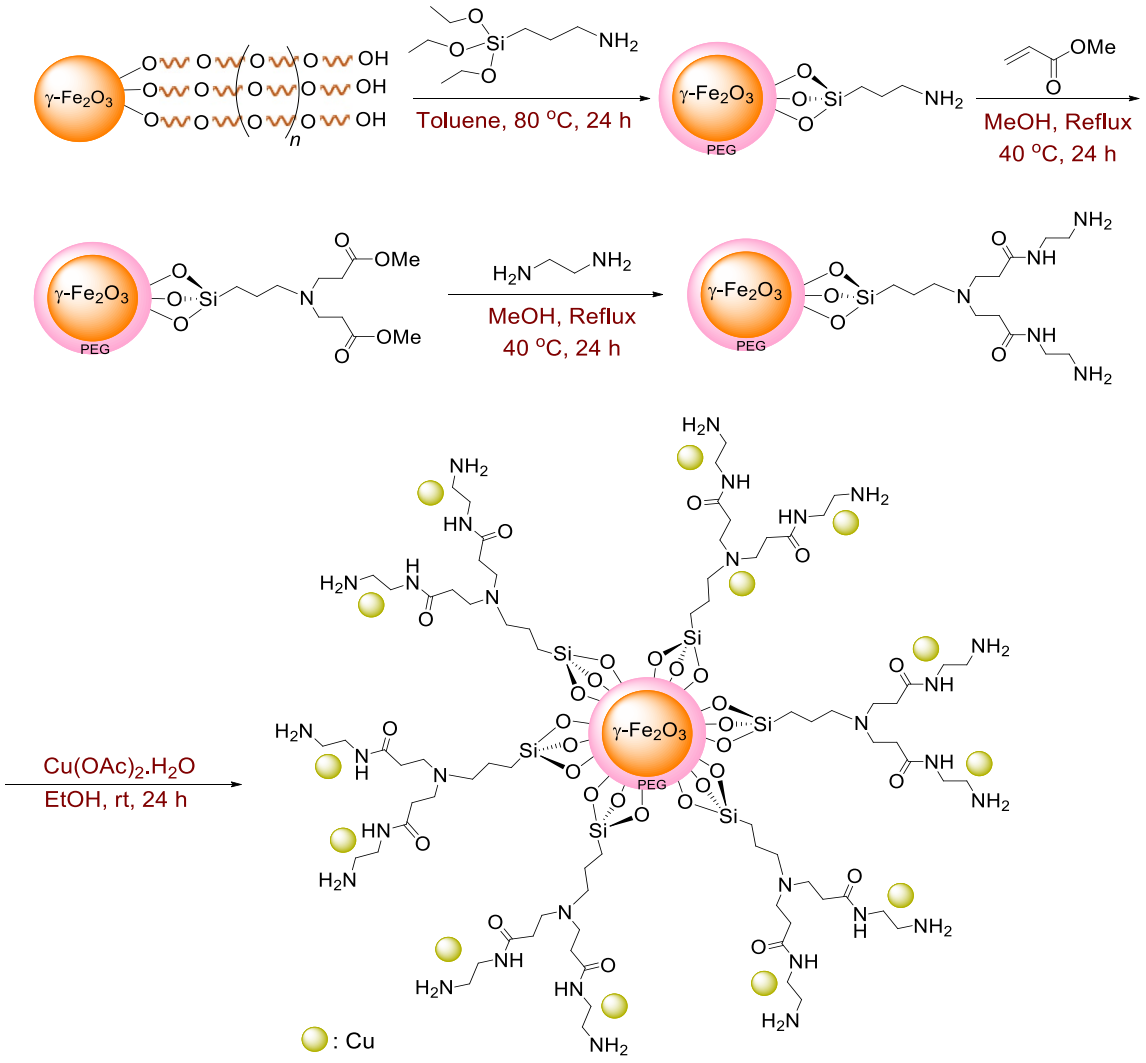

Figure 3. Preparation route for the catalyst, γ-Fe_2O_3@PEG@PAMAM G_0-Cu.

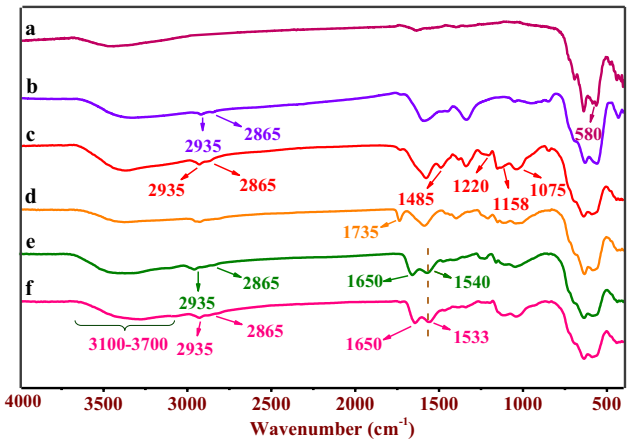

Figure 4. FT–IR spectra of the (**a**) γ–Fe_2O_3, (**b**) γ-Fe_2O_3@PEG, (**c**) γ-Fe_2O_3@PEG@APTES, (**d**) γ–Fe_2O_3@PEG@MAc, (**e**) γ-Fe_2O_3@PEG@PAMAM G_0, (**f**) γ-Fe_2O_3@PEG@PAMAM G_0-Cu.

raised to 50 °C and continued the reaction for 48 h. The ensued solid product was separated by an external magnet, washed with ethanol three times, and finally dried at 50 °C overnight to obtain γ-Fe_2O_3@PEG@PAMAM (1.09 gr).

Finally, the earlier prepared γ-Fe_2O_3@PEG@PAMAM MNPs (1 g) was dispersed in ethanol (30 mL) for 30 min, and then, $Cu(OAc)_2{\cdot}H_2O$ (0.199 g, 1 mmol) dissolved in ethanol (20 mL) was added to ethanolic dispersed mixture, while the reaction was stirred at 50 °C. Then, the reaction was allowed to proceed for 24 h. Finally, γ-Fe_2O_3@PEG@PAMAM-Cu (1.08 g) was obtained following the sequence of separation by an external magnet, washing with ethanol and after drying the particles in vacuum at 50 °C overnight (Fig. 3). ICP-OES analysis showed presence 0.96 mmol of Cu on 1 gr of γ-Fe_2O_3@PEG@PAMAM G_0-Cu (0.96 mmol, 0.06 gr, 0.25 wt%)).

General Procedure for the Sonogashira cross coupling reaction (1a-p). γ-Fe_2O_3@PEG@PAMAM G_0-Cu (0.8 mol%, 0.006 g) was added to a mixture of NaOH (2.0 mmol), phenylacetylene (1.5 mmol), and aryl halide (1.0 mmol) in water (5 mL), under stirring in air and heated at 80 °C. The progress of reaction was monitored by TLC until completion. After the completion of the reaction, the nanocatalyst was separated by an external magnet and washed with ethyl acetate (3 × 3 mL). The desired product (liquid phase) was extracted with ethyl acetate (3 × 6 mL), and the organic layers were dried over anhydrous Na_2SO_4. After evaporation of the solvent, crude product was purified by column or flash chromatography to afford the pure products **1a**-**p**.

Results and discussion

Preparation of γ-Fe_2O_3@PEG@PAMAM G_0-Cu. Initially, we selected γ-Fe_2O_3 MNPs as an attractive platform with unique features for the synthesis organic–inorganic heterogeneous catalyst. The preparation of γ-Fe_2O_3@PEG@PAMAM G_0-Cu as a water-soluble catalyst was pursued starting from divergent synthesis of PAMAM dendrimer zero generation using amino siloxy linker immobilized on the surface γ-Fe_2O_3@PEG MNPs, as the bivalence core ($-NH_2$). Eventually, deployment of $Cu(OAc)_2{\cdot}H_2O$, resulted in the preparation of the γ-Fe_2O_3@PEG@PAMAM G_0-Cu (Fig. 1). The catalyst structure was characterized via Fourier-transform infrared spectroscopy (FT-IR), transmission electron microscopy (TEM), X-ray diffraction analysis (XRD), field emission scanning electron microscopy (FE-SEM), inductively coupled plasma mass spectrometry (ICP), thermogravimetric analysis (TGA/DTG), value-stream mapping (VSM), MAP, nuclear magnetic resonance spectroscopy (NMR), and energy dispersive X-ray spectroscopy (EDX) (Figs. 4, 5, 6, 7, 8, 9, 10, 11, 12).

Characterization of the γ-Fe_2O_3@PEG@PAMAM G_0-Cu. Figure 4 presents the FT-IR spectra of the various synthetic segments of γ-Fe_2O_3@PEG@PAMAM G_0-Cu, comprising, γ-Fe_2O_3 (a), γ-Fe_2O_3@PEG (b), γ-Fe_2O_3@PEG@APTES (c), γ-Fe_2O_3@PEG@MAc (d), γ-Fe_2O_3@PEG@ PAMAM G_0 and (e), γ-Fe_2O_3@PEG@ PAMAM G_0-Cu (f). The strong absorption bond at about 580 cm^{-1} is assigned to the stretching vibrations of Fe–O in γ-Fe_2O_3 (Fig. 4a)[35,36]. The peak ~ 1075 cm^{-1} is attributed to the stretching of C–O bond of PEG (Fig. 4b)[37]. The absorption bands at 1055 and 1158 cm^{-1} are ascribed to the stretching vibrations of Si–O which demonstrates the appropriate functionalization of γ-Fe_2O_3 by APTES (Fig. 4b)[38,39]. The peak at 1735 cm^{-1} illustrates the stretching vibrations of the carbonyl group (C=O) in γ-Fe_2O_3@PEG@MAc (Fig. 4c)[40]. The peak at 1650 cm^{-1} elucidates the stretching vibrations of the carbonyl group (–CONH–) in γ-Fe_2O_3@PEG@PAMAM G_0 (Fig. 4c)[40]. Also, the absorption bond recorded for γ-Fe_2O_3@PEG@PAMAM G_0-Cu around 1540 cm^{-1} is attributed to the bending mode of N–H (Fig. 4c). Additionally, the bands corresponding to the asymmetric/symmetric aliphatic stretching modes of $-CH_2$ are represented in the regions 2935 and 2865 cm^{-1} (Fig. 4b–f)[41]. The broad band between 3100 and 3700 cm^{-1} corresponds to –NH and –OH stretching vibrations and a hydrogen bond (Fig. 4b–f)[41]. Also, the peak at 1485 cm^{-1} is ascribed to the bending of the ($-CH_2-$) bonds[42,43], whereas the peak around 1220 cm^{-1} is credited to the stretching vibrations of (C–N) bond (Fig. 4b,d)[44]. These results affirmed

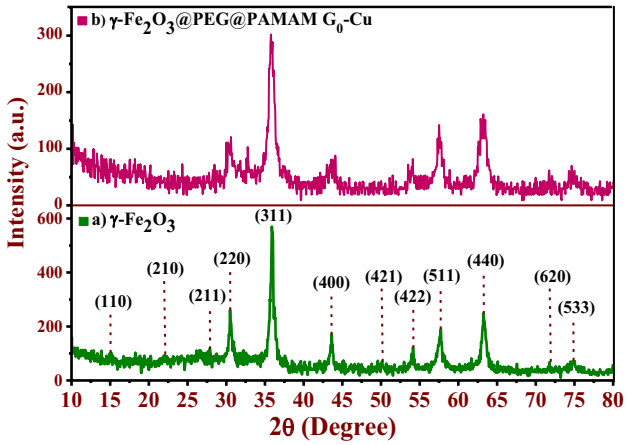

Figure 5. XRD patterns of (**a**) γ–Fe_2O_3, and (**b**) γ-Fe_2O_3@PEG@PAMAM G_0-Cu catalyst.

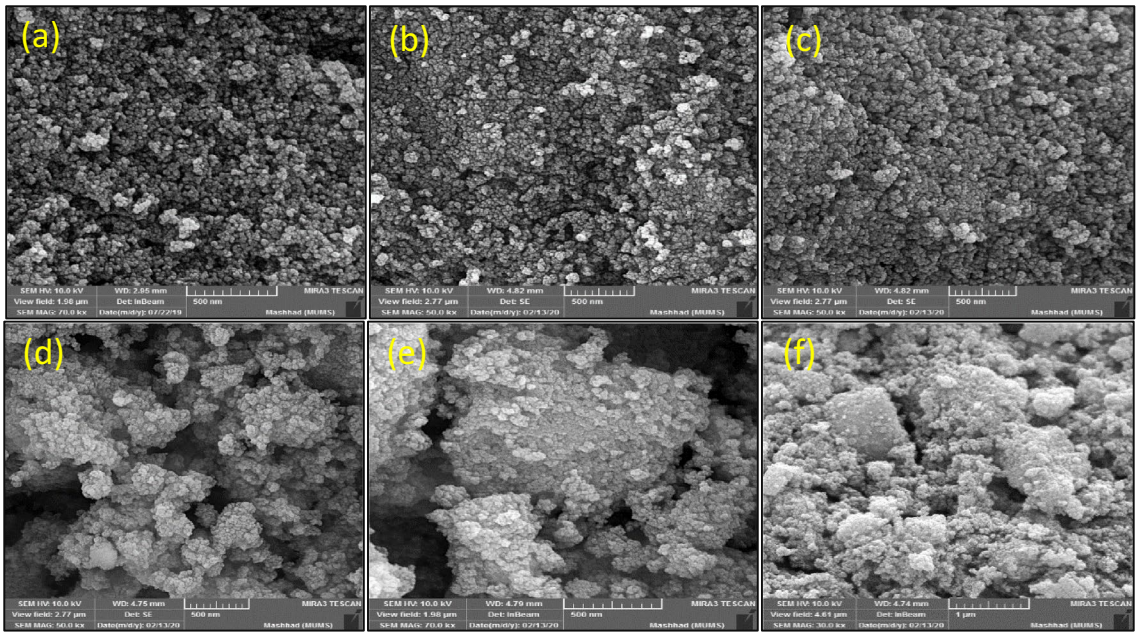

Figure 6. Field emission scanning electron microscopy pictures of the (**a**) γ–Fe_2O_3, (b) γ-Fe_2O_3@PEG, (**c**) γ-Fe_2O_3@PEG@APTES, (**d**) γ-Fe_2O_3@PEG@MAc, (**e**) γ-Fe_2O_3@PEG@PAMAM G_0, and (**f**) γ-Fe_2O_3@PEG@PAMAM G_0-Cu.

the successful preparation of the desired γ-Fe_2O_3@PEG@PAMAM G_0-Cu complex catalyst. Also, comparison of the FT-IR spectra of γ-Fe_2O_3@PEG@PAMAM G_0 and γ-Fe_2O_3@PEG@PAMAM G_0-Cu, showed the red shifting (~7 cm^{-1}) within the wavenumbers of stretching and bending modes of N–H indicating that the Cu is coordinated on the surface of the nitrogen atoms of γ-Fe_2O_3@PEG@PAMAM G_0 (Fig. 4c,d). These results confirmed the successful preparation of the γ-Fe_2O_3@PEG@PAMAM G_0-Cu MNPs.

The XRD patterns of the purity γ-Fe_2O_3 and γ-Fe_2O_3@PEG@PAMAM G_0-Cu catalyst is depicted in Fig. 5. The diffractogram of γ-Fe_2O_3 indicated several diffraction main peaks at 15°, 23.1°, 26.9°, 30.3°, 35.8°, 43.6°, 50°, 54.8°, 57.3°, 63.2°, 71.1°, and 74.4° (2θ), corresponded respectively to the (110), (210), (211), (220), (311), (400), (421), (422), (511), (440), (620), and (533) miller indices, that confirms with cubic magnetite crystal structure according to data base peaks (JCPDS card No. 39-1346) (Fig. 5a)[45,46]. As shown in XRD pattern of the γ-Fe_2O_3@PEG@PAMAM G_0-Cu, crystalline phase and peaks location of this pattern also exhibit cubic structure and displayed the similar diffraction peaks to those of the pattern pertinent γ-Fe_2O_3. Further, in XRD pattern of γ-Fe_2O_3@PEG@PAMAM G_0-Cu, decreasing of peaks intensity in comparison to γ-Fe_2O_3 is clearly visible which is due to the functionalization of maghemite NPs with various groups and Cu complex formation (Fig. 5b). The crystallite size of γ-Fe_2O_3@PEG@PAMAM G_0-Cu catalyst was determined by using Williamson-Hall equation: $\beta \cdot \cos\theta = (K\lambda)/D + \eta \cdot \sin\theta$. According to the Williamson-Hall plot, with 0% strain the particle size was found 11.4 nm (114 Å) (ESI, Fig. S1).

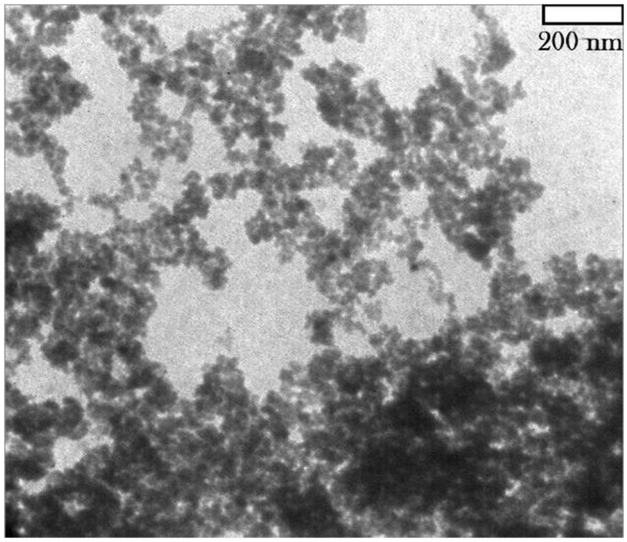

Figure 7. Transmission electron microscopy (TEM) picture of γ-Fe_2O_3@PEG@PAMAM G_0-Cu catalyst.

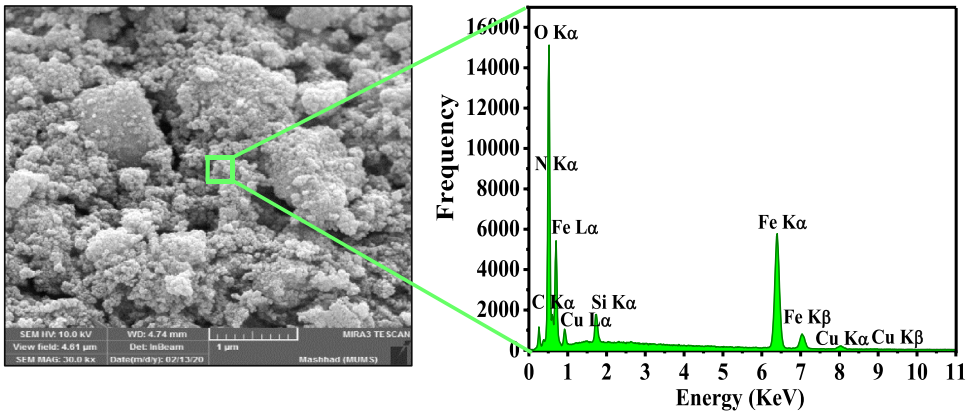

Figure 8. EDX analysis of the γ-Fe_2O_3@PEG@PAMAM G_0-Cu catalyst.

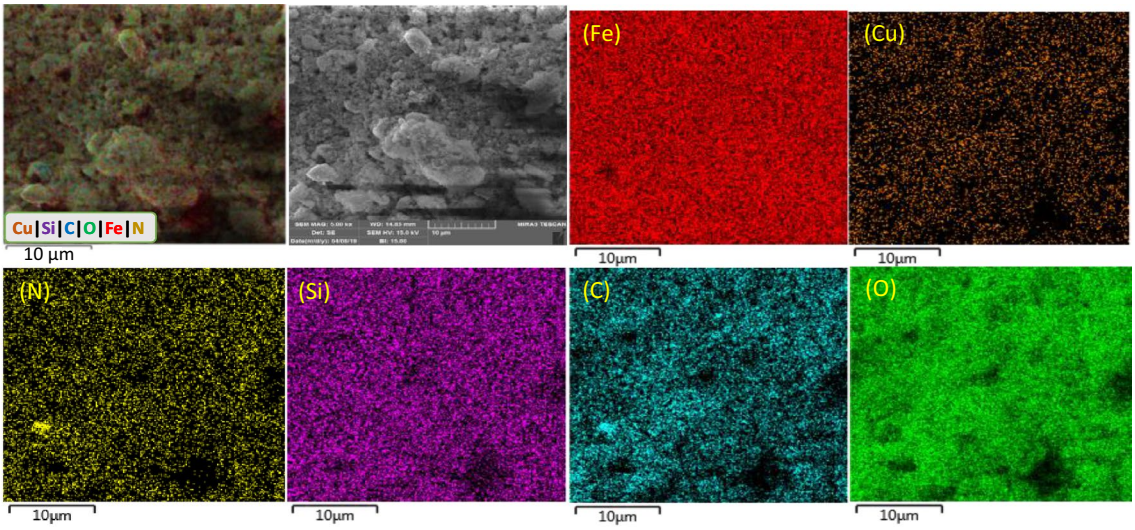

Figure 9. EDS elemental mappings of the γ-Fe_2O_3@PEG@PAMAM G_0-Cu catalyst.

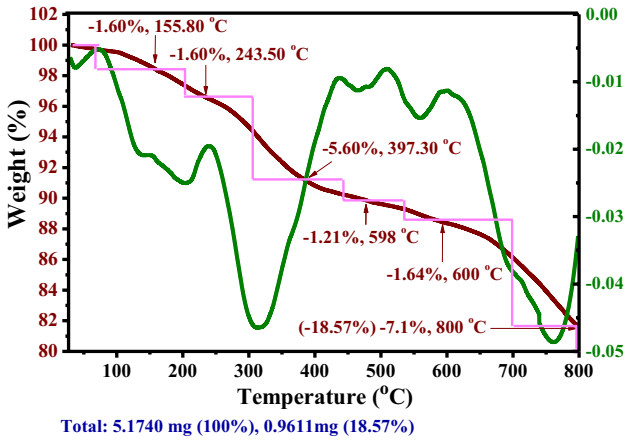

Figure 10. TGA/DTG/DTA weight loss curves of the γ-Fe_2O_3@PEG@PAMAM G_0-Cu.

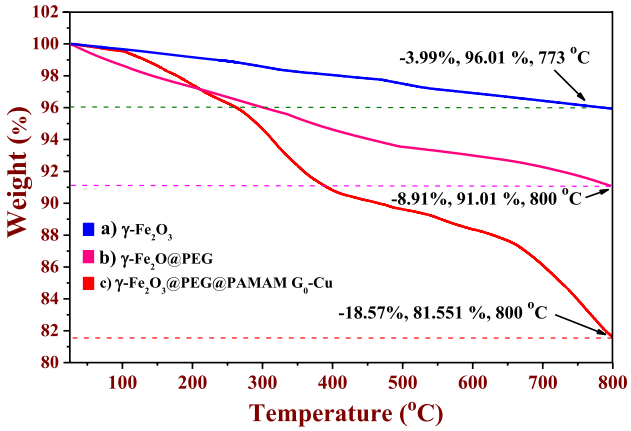

Figure 11. TGA weight loss curves of the (**a**) γ-Fe_2O_3 (**b**) γ-Fe_2O_3@PEG (**c**) γ-Fe_2O_3@PEG@PAMAM G_0-Cu.

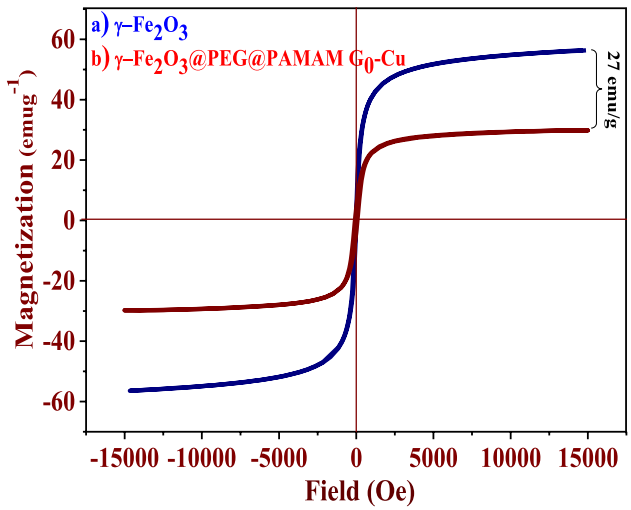

Figure 12. Magnetization curves of (**a**) γ-Fe_2O_3, (**b**) γ-Fe_2O_3@PEG@PAMAM G_0-Cu at 300 K.

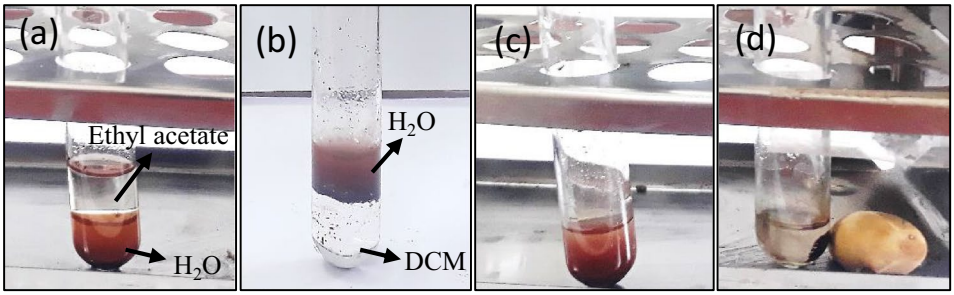

Figure 13. (**a**) Distribution of γ-Fe_2O_3@PEG@PAMAM G_0-Cu in biphasic H_2O-ethyl acetate, (**b**) distribution of γ-Fe_2O_3@PEG@PAMAM G_0-Cu in biphasic H_2O-dichloromethane (DCM), (**c**) dispersion of γ-Fe_2O_3@PEG@PAMAM G_0-Cu in H_2O, (**d**) easy separation of γ-Fe_2O_3@PEG@PAMAM G_0-Cu using an external magnet.

Scanning electron microscopy (SEM) investigation was also performed to study the surface and cross sectional morphology of the corresponding the preparation various parts of Cu catalyst, including, γ-Fe_2O_3 (a), γ-Fe_2O_3@PEG (b), γ-Fe_2O_3@PEG@APTES (c), γ-Fe_2O_3@PEG@MAc (d), γ-Fe_2O_3@PEG@PAMAM G_0 (e), γ-Fe_2O_3@PEG@PAMAM G_0-Cu (f), with scale bar 200 nm (Fig. 6a–f). The results of all SEM micrographs of the preparation various parts of γ-Fe_2O_3@PEG@PAMAM G_0-Cu complex, clearly reveal the homogeneous spherical morphology and uniform size distribution (Fig. 6a–f). Also, the morphology of the γ-Fe_2O_3@PEG@PAMAM G_0-Cu complex were monitored by transmission electron microscopy (TEM) (Fig. 5a). TEM picture clearly shows the small sized spherical structure without significant agglomeration phenomena for the γ-Fe_2O_3@PEG@PAMAM G_0-Cu MNPs (Fig. 7a). Also, the average particle size of the adsorbed copper catalyst was 12 nm based on the TEM images (ESI, Fig. S2).

The EDX analysis results confirmed that γ-Fe_2O_3@PEG@PAMAM G_0-Cu complex encompass the Cu, N, C, O, Si, and Fe elements, as expected (Fig. 8). In additional, EDS elemental mapping of γ-Fe_2O_3@PEG@PAMAM G_0-Cu, confirmed presence all expected elements including Fe, N, C, Si, Cu, O, and shows that Cu is homogeneously distributed on the γ-Fe_2O_3@PEG@PAMAM G_0-Cu (Fig. 9).

The loading of the Cu amount on catalyst was determined by ICP-OES analysis which according to the results amount of copper incorporated on 1.0 g of γ-Fe_2O_3@PEG@PAMAM G_0-Cu complex was determined to be 0.96 mmol.

The TGA curve of γ-Fe_2O_3@PEG@PAMAM G_0-Cu showed weight loss at five stages, totaling 18.57% that demonstrate the good thermal stability of γ-Fe_2O_3@PEG@PAMAM G_0-Cu, at a heating rate of 10 °C min^{-1} in the temperature range of 25–800 °C under nitrogen atmosphere (Fig. 10).

The first weight loss is attributed to the removal of trapped water content in the crystalline structure of the Cu complex (− 1.60 W%, ~ 150 °C) (Fig. 10). The second to fifth weight loss of γ-Fe_2O_3@PEG@PAMAM G_0-Cu were observed in the regions 243–600 °C (− 1.60, − 5.60, − 1.21, and − 1.64 W%) which are attributed to decomposition of the organic compounds grafted on the surface of γ-Fe_2O_3, including, PEG, amino-siloxy linker, and PAMAM dendrimer (Fig. 10). The weight loss, in the temperature range of 800 °C (− 7.10 W%) probably are related to the removal of PEG and N_2, CO_2 gases, and as well as mineral impurities in the γ-Fe_2O_3 (Fig. 10).

Also, for better comprehension of the thermal behavior of γ-Fe_2O_3@PEG@PAMAM G_0-Cu, the thermogravimetric analysis results were compared for γ-Fe_2O_3, γ-Fe_2O_3@PEG and γ-Fe_2O_3@PEG@PAMAM G_0-Cu compounds (Fig. 11). Based on the results of thermogram curves depicted in Fig. 11, of the total weight loss for the γ-Fe_2O_3@PEG@PAMAM G_0-Cu (− 18.57 w%) in the temperature range of 25–800 °C, ~ − 3.99 W%, is attributed to the mineral impurities in the γ-Fe_2O_3 MNPs, and ~ − 4.92 W% is attributed to decomposition of PEG (Fig. 11).

The magnetic properties of γ-Fe_2O_3 MNPs and γ-Fe_2O_3@PEG@PAMAM G_0-Cu complex were evaluated using the vibrating sample magnetometer analysis (VSM) at 25 °C (Fig. 12). According to the VSM results, the magnetization for γ-Fe_2O_3 MNPs was found around 55 emu g^{-1}, which revealed the superparamagnetic property (Fig. 12a). After functionalization of γ-Fe_2O_3 to prepare γ-Fe_2O_3@PEG@PAMAM G_0-Cu, this value dropped to 27 emu g^{-1} (Fig. 12b) thus confirming the successful functionalization of the γ-Fe_2O_3 MNPs and the formation of Cu complex (Fig. 12).

Evaluation of the catalytic activity of γ-Fe_2O_3@PEG@PAMAM G_0-Cu MNPs. Subsequent to the characterization and structural confirmation of the γ-Fe_2O_3@PEG@PAMAM G_0-Cu, the Sonogashira C–C cross coupling reaction was explored for assessing its performance and reactivity in aqueous medium as a green solvent, the main objective of our strategy being to provide an active catalyst in water as an ideal alternative to conventional organic solvents for performing such coupling reactions. Figure 13 clearly show the hydrophilic properties of γ-Fe_2O_3@PEG@ PAMAM G_0-Cu catalyst.

Optimization study for the Sonogashira cross-coupling reaction. In this section, the optimal reaction conditions were explored for the Sonogashira cross-coupling reaction, using γ-Fe_2O_3@PEG@PAMAM G_0-Cu as a hydrophilic catalyst. To this end, phenylacetylene and aryl iodide were selected as model substrates to identify appropriate parameters on the progress of the target reaction. Thus, the effect of temperature changes,

Entry	Catalyst (mol%)	Base (mmol)	T (°C)	Time (h)	Isolated yield (%)[a]
1	0.8	K_2CO_3 (2)	80	3	50
2	0.8	Et_3N (2)	80	3	68
3	0.8	NaOH (2)	80	3	94
4	0.8	KOH (2)	80	3	86
5	0.8	NaOH (2)	r.t	12	Trace
6	0.8	NaOH (2)	60	3	80
7	0.4	NaOH (2)	80	3	65
8	0.8	NaOH (1)	80	3	70
9	0.8	NaOH (3)	80	3	94
10	0.8	–	80	3	–

Table 1. Optimization reaction condition of Sonogashira coupling of iodobenzene and phenylacetylene catalyzed by γ-Fe_2O_3@PEG@PAMAM G_0-Cu in the water under different conditions. [a]Reaction conditions: iodobenzene (1.00 mmol), phenylacetylene (1.5 mmol), H_2O (5.0 mL).

amount of catalyst loading, type and amount of base used, on the model reaction was discerned (Table 1, entries 1–10). Initially, 0.8 mol% of Cu complex was exposed to model substrates and 2 mmol of various base (K_2CO_3, Et_3N, NaOH, KOH) in water as a green solvent (5.0 mL), in pure water, at 80 °C (Table 1, entries 1–4). When the reaction was performed using K_2CO_3, Et_3N bases (Table 1, entries 1 and 2), formation of 1,2-diphenylacetylene product **1a** reached to 50 and 68% yields, respectively. Also, changing the type of base to KOH resulted in an improved yield of **1a** (Table 1, 86%, entry 4). Best result was obtained for the formation of **1a**, deploying NaOH (94%, entry 3) as a base. Subsequently, the effect of temperature changes was examined on advancing the model reaction (Table 1, entries 5 and 6). In this series of experiments, the model reaction could be performed at the room temperature, even after 12 h of continuous reaction, no product was obtained (Table 1, trace, entry 5). Also, decreasing the temperature to 60 °C led to incomplete production (Table 1, 80%, entry 6). Best result was obtained at 80 °C that led to 94% formation of **1a** (Table 1, entry 3). In the next stage, amount loading of Cu catalyst was assessed where the ideal result was found to relate to 0.8 mol% loading of the catalyst (0.8 mol% of Cu, 0.006 g of Cu catalyst) that led to formation of biphenyl product **1a** in 94% yield (Table 1, entry 3). Furthermore, in the absence of NaOH as a base, no product was obtained (Table 1, entry 10). Decreasing the amount of base used (NaOH, 1 mol) also did not have a favorable effect, which afforded moderate conversion of **1a** (70%, entry 8). Also, increase the amount of base used (NaOH, 3 mol) also was not effective in progressing the model reaction (Table 1, 94%, entry 9). In general, the best results were found using 0.8 mol% loading of the γ-Fe_2O_3@PEG@PAMAM G_0-Cu catalyst (0.006 g), NaOH as a base (2 mmol), in H_2O (5 mL) at 80 °C for 180 min giving compound **1a** in 94% isolated yield (see Table 1 for more details).

Substrate scope. To the overall performance appraisement and to ascertain the limitation of Sonogashira reaction using γ-Fe_2O_3@PEG@PAMAM G_0-Cu catalyst, a series of assorted aryl iodides and aryl bromides were examined in reaction with phenylacetylene under the optimal reaction conditions (0.8 mol% of Cu catalyst with NaOH, in pure water, at 80 °C, see Table 2). As depicted in the Table 2, a broad range of 1,2-diphenylacetylene products were synthesized, emanating from both, the aryl bromide and aryl iodide substituted with electron-donating (–NH_2, –OMe, –Me) and electron-withdrawing functional groups (Cl, –CO_2Me, –COMe, –CN, –NO_2) and affording good to excellent yields (45–90%). However, the results related to aryl iodides (55–94%) were better than aryl bromide (45–80%), I > Br. In general, the results of using γ-Fe_2O_3@PEG@PAMAM G_0-Cu for Sonogashira cross coupling reactions to the corresponding 1,2-diphenylacetylene products, were encouraging which led to the production a range of 1,2-diphenylacetylene products (see Table 2 entries 1a–p for additional details).

Experimental controls. To demonstrate the catalytic role and uniqueness of the nano γ-Fe_2O_3@PEG@PAMAM G_0-Cu complex, some control experiments were conducted for the model reaction of Sonogashira (Fig. 14). For this goal, the model reaction was performed and compared using the parent materials. The results clearly indicated the high activity and efficiency of the γ-Fe_2O_3@PEG@PAMAM G_0-Cu catalyst, compared to the other examined catalysts (Fig. 14).

Recyclability study. Recyclability aspects of the γ-Fe_2O_3@PEG@PAMAM G_0-Cu catalyst complex were evaluated for model reaction to achieve of **1a**, under the optimized reaction conditions for 6 serial runs (see Table 3). According to the obtained results, the highly activated catalyst represented just 0–1% loss of efficiency after the 6 successive runs for preparation of **1a** (Table 3).

In addition, FT–IR analysis was performed for the γ-Fe_2O_3@PEG@PAMAM G_0-Cu catalyst used after the 6th runs in the model reaction (see Fig. 15a,b). Study of the FT–IR spectra related to 6th runs of catalyst, demonstrate the stability structure of the catalyst that have been retained after 6th recovery in the model reaction (see Fig. 15).

The comparison of TEM and SEM images of fresh copper catalyst and the used catalyst after 6th run in the model reaction, did not reveal any detectable and noticeable change in size and morphology (Fig. 16A, B). Moreover, a good dispersion and small NPs of Cu-complex even after six recovering times, is related to the stability of

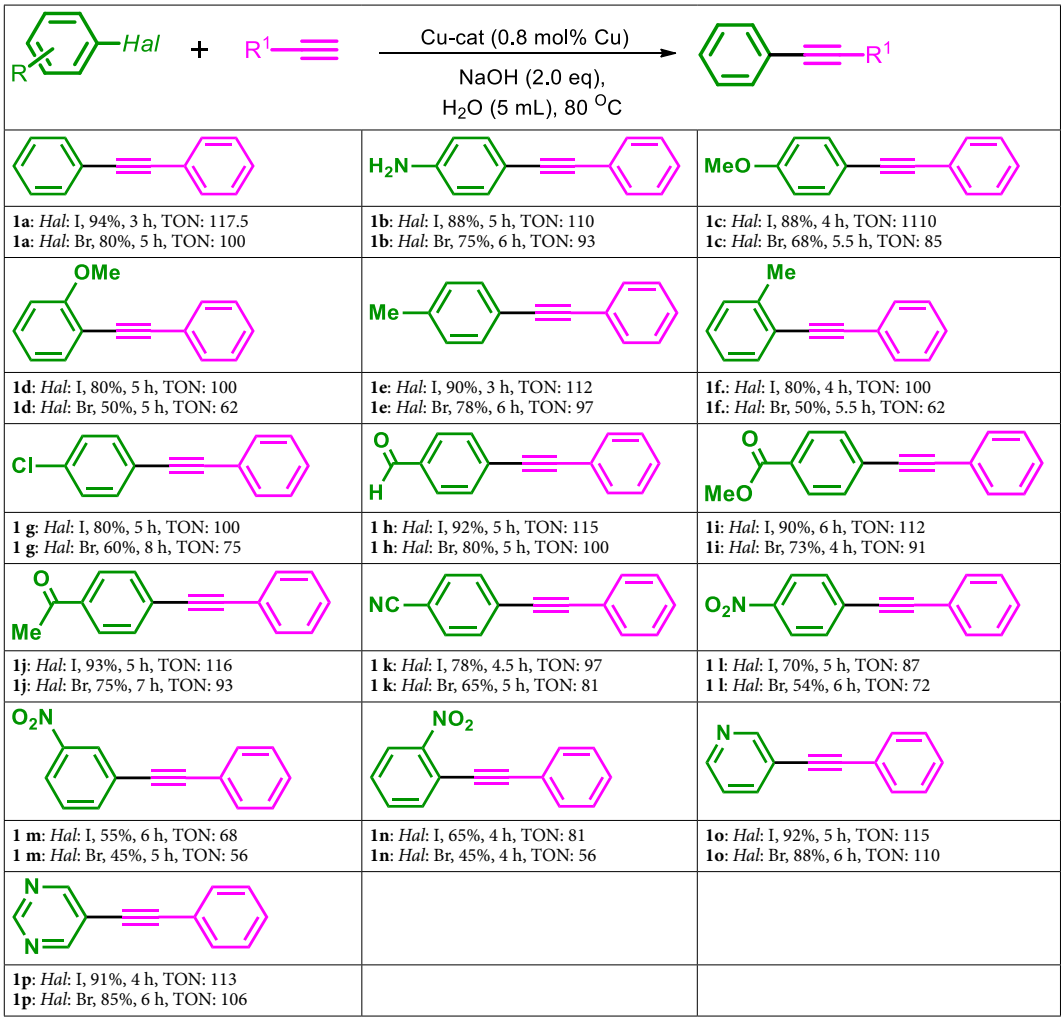

1a: *Hal*: I, 94%, 3 h, TON: 117.5 **1a**: *Hal*: Br, 80%, 5 h, TON: 100	**1b**: *Hal*: I, 88%, 5 h, TON: 110 **1b**: *Hal*: Br, 75%, 6 h, TON: 93	**1c**: *Hal*: I, 88%, 4 h, TON: 1110 **1c**: *Hal*: Br, 68%, 5.5 h, TON: 85
1d: *Hal*: I, 80%, 5 h, TON: 100 **1d**: *Hal*: Br, 50%, 5 h, TON: 62	**1e**: *Hal*: I, 90%, 3 h, TON: 112 **1e**: *Hal*: Br, 78%, 6 h, TON: 97	**1f.**: *Hal*: I, 80%, 4 h, TON: 100 **1f.**: *Hal*: Br, 50%, 5.5 h, TON: 62
1 g: *Hal*: I, 80%, 5 h, TON: 100 **1 g**: *Hal*: Br, 60%, 8 h, TON: 75	**1 h**: *Hal*: I, 92%, 5 h, TON: 115 **1 h**: *Hal*: Br, 80%, 5 h, TON: 100	**1i**: *Hal*: I, 90%, 6 h, TON: 112 **1i**: *Hal*: Br, 73%, 4 h, TON: 91
1j: *Hal*: I, 93%, 5 h, TON: 116 **1j**: *Hal*: Br, 75%, 7 h, TON: 93	**1 k**: *Hal*: I, 78%, 4.5 h, TON: 97 **1 k**: *Hal*: Br, 65%, 5 h, TON: 81	**1 l**: *Hal*: I, 70%, 5 h, TON: 87 **1 l**: *Hal*: Br, 54%, 6 h, TON: 72
1 m: *Hal*: I, 55%, 6 h, TON: 68 **1 m**: *Hal*: Br, 45%, 5 h, TON: 56	**1n**: *Hal*: I, 65%, 4 h, TON: 81 **1n**: *Hal*: Br, 45%, 4 h, TON: 56	**1o**: *Hal*: I, 92%, 5 h, TON: 115 **1o**: *Hal*: Br, 88%, 6 h, TON: 110
1p: *Hal*: I, 91%, 4 h, TON: 113 **1p**: *Hal*: Br, 85%, 6 h, TON: 106		

Table 2. Sonogashira coupling reactions of different aryl halides with phenylacetylene catalyzed by γ-Fe_2O_3@PEG@PAMAM G_0-Cu[a]. [a]Reaction conditions: aryl halide (1.00 mmol), acetylene (1.5 mmol), NaOH (2.00) mmol, catalyst (0.006 g, 0.8 mol% Cu), H_2O (5.0 mL), 80 °C; All yields are isolated.

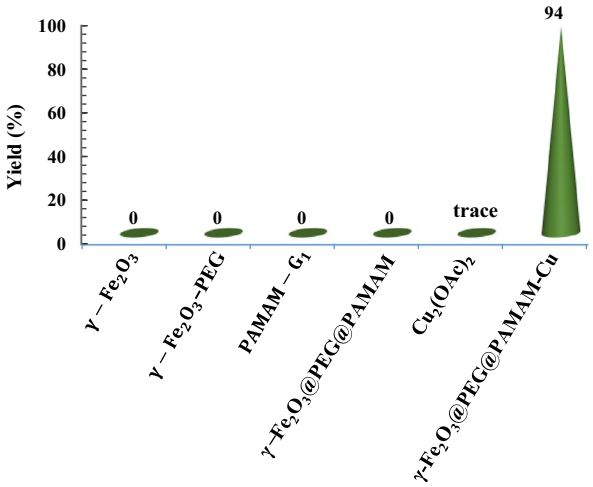

Figure 14. Control experiments to show the catalytic activity of the γ-Fe_2O_3@PEG@PAMAM G_0-Cu for the Sonogashira model reaction.

Run[a]	Yield (%)	Time (h)	TON
1	94	3	177
2	94	3	177
3	94	4	177
4	93	4	116
5	93	4	116
6	93	5	116

Table 3. Recyclability of the γ-Fe_2O_3@PEG@PAMAM G_0-Cu catalyst in performed of the Sonogashira reaction[a]. [a]Reaction conditions: iodobenzene (1.00 mmol), phenylacetylene (1.5 mmol), NaOH (2.00 mmol), catalyst (0.8 mol% of Cu, 0.006 g), H_2O (5.0 mL), 80 °C.

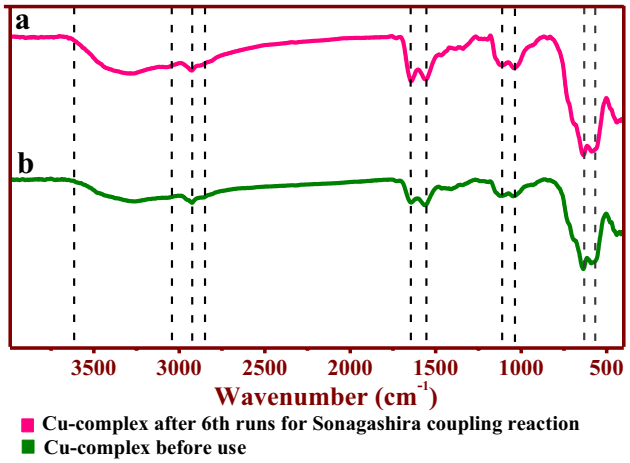

Figure 15. FT−IR spectra of (**a**) γ-Fe_2O_3@PEG@PAMAM-Cu, before use; (**b**) γ-Fe_2O_3@PEG@PAMAM G_0-Cu catalyst after 6th runs for the model reaction.

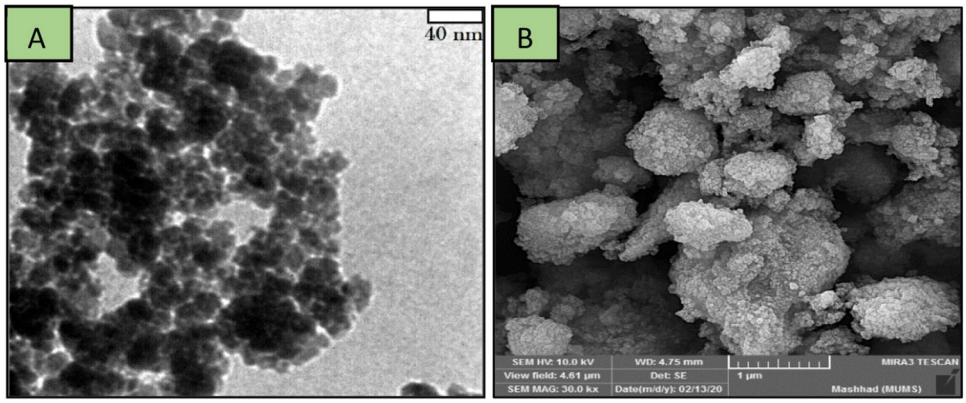

Figure 16. (**A**) TEM, and (**B**) FE – SEM, images recovered of the γ-Fe_2O_3@PEG@PAMAM G_0-Cu complex after the 6th run for model reaction, reaction conditions: iodobenzene (1.00 mmol), phenylacetylene (1.5 mmol), NaOH (2.0 mmol), catalyst (0.8 mol% of Cu, 0.006 g), H_2O (5.0 mL), 80 °C.

the γ-Fe_2O_3@PEG@PAMAM G_0-Cu catalyst. However, minimal agglomeration can be seen in the TEM image that is associated with the dipole–dipole interactions of magnetic nano particles (Fig. 16A, B).

ICP analysis was performed for measurement of the copper leaching for the six catalytic run steps of model reaction (Fig. 17). ICP analysis results of Cu complex after the 6th run demonstrated a stable catalytic structure with a small amounts of Cu leaching (average up to 2.4%) (Fig. 17).

Moreover, a rigorous investigation was conducted to elucidate the stability and heterogeneous nature of the catalyst using the hot-filtration method on the model reaction (ESI, Fig. S3). After the catalyst was magnetically

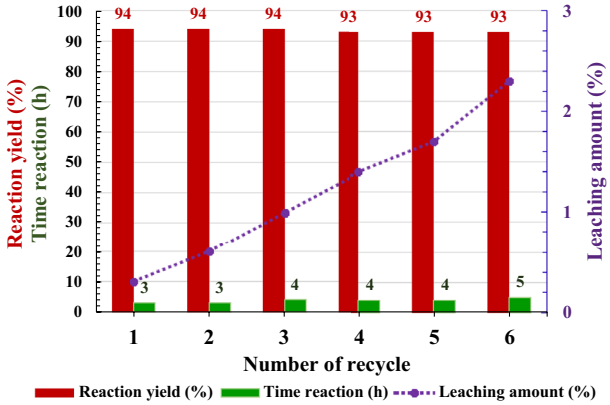

Figure 17. Determination, amount metal leaching of the Cu catalyst during 6th runs of the model reaction, in optimal reaction conditions; reaction conditions: iodobenzene (1.00 mmol), phenylacetylene (1.5 mmol), NaOH (2.0 mmol), catalyst (0.006 g, 0.8 mol% of Cu), H_2O (5.0 mL), 80 °C.

Entry	Catalyst (mol%)	Reaction conditions	Time (h)	Yield[b] (%)	Refs.
1	CuI (0.2 mol%)	K_2CO_3/PPh_3 (4 mol%)/H_2O/140 °C	24	43	[47]
2	NHC precursor (20 mol%)/$CuSO_4{\cdot}5H_2O$ (20 mol%)[c]	K_2CO_3/DMF/125 °C	8	71	[48]
3	$Co(C_9H_9NO_2)_3$	K_2CO_3/DMF/ethylene glycol/r.t	8	82	[49]
4	MNPs@Cs-MS-Co (0.55 mol%)[d]	KOH/DMSO/140 °C	10	72	[50]
5	CuO/TiO_2	K_2CO_3/EtOH/r.t	15	54	[51]
6	Pd_3Cu_1/SiC	Cs_2CO_3/DMF/60 °C	8	99	[52]
7	$Cu(OAc)_2$ (10 mol%)/β-diketone	K_2CO_3/DMF/120 °C	36	90	[53]
8	Cu-Salen (10 mol%)/PTC[e]	NaOH/H_2O/100 °C	24	76	[54]
9	Cu (10 mol%)/DABCO@SiO	KOH/DMF/140 °C	2	94	[55]
10	γ-Fe_2O_3@PEG@PAMAM G_0-Cu	NaOH/H_2O/80 °C	3	94	This work

Table 4. Catalytic activity of the γ-Fe_2O_3@PEG@PAMAM G_0-Cu MNPs was compared with reported catalysts for the Sonogashira cross coupling reaction (1a)[a]. [a]Sonogashira: reaction of iodobenzene and phenyl acetylene. [b]Isolated yield. [c]NHC: N-heterocyclic carbine. [d]MNPs@Cs-MS-Co: cobalt tagged on MNPs-chitosan functionalized with methyl salicylate. [e]PTC: phase-transfer catalyst.

removed from the reaction medium (t = 70 min, 46% yield of 1,2-diphenylacetylene monitored by GC), and the reactants were allowed to undergo further reaction, when the reaction did not progress (49% yield after 180 min, Fig. S3). This confirmed that the catalyst functioned heterogeneously in the reaction and consequently only slight leaching occurred during the reaction.

Catalytic performance. Catalytic efficiency of the γ-Fe_2O_3@PEG@PAMAM G_0-Cu complex in terms of the reaction time, and yield was compared with the other reported catalysts for the Sonogashira reaction (see Table 4). The high activity of the catalyst in water media, as an abundant, and available solvent is notable. Additional benefits of this catalytic methodology in comparison with the others catalytic protocols are presented in Table 4 are the simplicity of catalyst separation, higher yield of the corresponding products during the shorter reaction times, eco-friendly and economic aspects, as well as the use of available and inexpensive copper metal complex (see Table 4. For more details).

Summary and conclusions

In brief, we have developed an environmentally friendly and economical methodology using a water-dispersible, recyclable copper catalyst (γ-Fe_2O_3@PEG@PAMAM G_0-Cu) based on the γ-Fe_2O_3 nanoparticles coated with polyethylene glycol to promote the Sonogashira coupling reaction in water as a solvent. The physicochemical properties of γ-Fe_2O_3@PEG@PAMAM G_0-Cu catalyst were characterized using various techniques such as, FT-IR, FE-SEM, XRD, VSM, EDS, TGA and TEM analysis. Polyethylene glycol on the surface of iron oxide nanoparticles instigated the good dispersion of the catalyst in the aqueous media and thus increased the interaction between the precursor materials and the catalyst like homogeneous systems. A wide range of aryl halides (aryl iodide and aryl bromide) reacted with phenylacetylene using copper catalyst in the water and led to attainment of the desired products with good to excellent efficiencies. The easy recyclability of the catalyst using an external

magnet and its reusability, as well as the good performance of the catalyst in water solvent without the use of additives such as alcohol or added surfactant are other salient advantages of this developed catalyst.

Data availability

All data generated or analyzed during this study are included in this published article [and its supplementary information files].

Received: 26 July 2022; Accepted: 17 October 2022
Published online: 26 October 2022

References

1. Zimmerman, J. B., Anastas, P. T., Erythropel, H. C. & Leitner, W. Designing for a green chemistry future. *Science* **367**, 397–400 (2020).
2. Thathagar, M. B., Beckers, J. & Rothenberg, G. Palladium-free and ligand-free Sonogashira cross-coupling. *Green Chem.* **6**, 215–218 (2004).
3. Chen, T. L. *et al.* Implementation of green chemistry principles in circular economy system towards sustainable development goals: Challenges and perspectives. *Sci. Total Environ.* **716**, 136998 (2020).
4. Zhang, W. & Cue, B. W. *Green Techniques for Organic Synthesis and Medicinal Chemistry* (Wiley, 2018).
5. Destito, P., Vidal, C., López, F. & Mascareñas, J. L. Transition metal-promoted reactions in aqueous media and biological settings. *Chem. Eur. J.* **27**, 4789–4816 (2021).
6. C. M. Eichenseer, B. Kastl, M. A. Pericàs, P. R. Hanson & O. Reiser. *ACS Sustain. Chem. Eng.* **4**, 2698-2705 (2016).
7. Baig, R. N. & Varma, R. S. Magnetically retrievable catalysts for organic synthesis. *ChemComm.* **49**, 752–770 (2013).
8. Baig, R. N. & Varma, R. S. Organic synthesis via magnetic attraction: Benign and sustainable protocols using magnetic nanoferrites. *Green Chem.* **15**, 398–417 (2013).
9. Joshi, R. *et al.* Ningthoujam, insights into the structural and microscopic origin of magnetic properties of the γ-Fe_2O_3@MnxOy nanostructure. *J. Phys. Chem. C.* **125**, 17971–17982 (2021).
10. Simon, M. O. & Li, C. J. Green chemistry oriented organic synthesis in water. *Chem. Soc. Rev.* **41**, 1415–1427 (2012).
11. Li, C.-J. & Chen, L. Organic chemistry in water. *Chem. Soc. Rev.* **35**, 68–82 (2006).
12. Nasrollahzadeh, M. *et al.* Recent advances in polymer supported palladium complexes as (nano) catalysts for Sonogashira coupling reaction. *Mol. Catal.* **480**, 110645 (2020).
13. Shin, H., Suh, Y. & Lim, D. Recent progress in plasmonic hybrid photocatalysis for CO_2 photoreduction and C–C coupling reactions. *Catalysts* **11**, 155 (2021).
14. Lee, N. R. *et al.* A low-foaming surfactant for organic synthesis in water. *Chemsuschem* **12**, 3159–3165 (2019).
15. Nasseri, M. A., Rezazadeh, Z., Kazemnejadi, M. & Allahresani, A. A Co–Cu bimetallic magnetic nanocatalyst with synergistic and bifunctional performance for the base-free Suzuki, Sonogashira, and C–N cross-coupling reactions in water. *Dalton Trans.* **49**, 10645–10660 (2020).
16. Parandhaman, T., Pentela, N., Ramalingam, B., Samanta, D. & Das, S. K. Metal nanoparticle loaded magnetic-chitosan microsphere: Water dispersible and easily separable hybrid metal nano-biomaterial for catalytic applications. *ACS Sustain. Chem. Eng.* **5**, 489–501 (2017).
17. Motahharifar, N., Nasrollahzadeh, M., Taheri-Kafrani, A., Varma, R. S. & Shokouhimehr, M. Magnetic chitosan-copper nanocomposite: A plant assembled catalyst for the synthesis of amino-and N-sulfonyl tetrazoles in eco-friendly media. *Carbohydr. Polym.* **232**, 115819 (2020).
18. Baig, R. N. & Varma, R. S. Copper on chitosan: A recyclable heterogeneous catalyst for azide–alkyne cycloaddition reactions in water. *Green Chem.* **15**, 1839–1843 (2013).
19. Vaddula, B. R., Saha, A., Varma, R. S. & Leazer, J. Tsuji-Trost N-allylation with allylic acetates by using a cellulose-palladium catalyst. *Eur. J. Org. Chem.* **2012**, 6707–6709 (2012).
20. Kou, J., Saha, A., Bennett-Stamper, C. & Varma, R. S. Inside-out core–shell architecture: controllable fabrication of Cu_2O@Cu with high activity for the Sonogashira coupling reaction. *ChemComm.* **48**, 5862–5864 (2012).
21. Yuan, Y., Zhu, H., Zhao, D. & Zhang, L. Ligand-free copper oxide nanoparticle-catalyzed sonogashira coupling reaction. *Synthesis* **2011**, 1792–1798 (2011).
22. Biffis, A., Scattolin, E., Ravasio, N. & Zaccheria, F. Supported copper precatalysts for ligand-free, palladium-free Sonogashira coupling reactions. *Tetrahedron Lett.* **48**, 8761–8764 (2007).
23. Arundhathi, R., Damodara, D., Mohan, K. V., Kantam, M. L. & Likhar, P. R. Monodispersed and stable nano copper (0) from copper-aluminium hydrotalcite: Importance in C–C couplings of deactivated aryl chlorides. *Adv. Synth. Catal.* **355**, 751–756 (2013).
24. Mitrofanov, A. Y., Murashkina, A. V., Martín-García, I., Alonso, F. & Beletskaya, I. P. Formation of C-C, C–S and C–N bonds catalysed by supported copper nanoparticles. *Catal. Sci. Technol.* **7**(19), 4401–4412 (2017).
25. Al-Zoubi, R. M., Al-Omari, M. K., Al-Jammal, W. K. & Ferguson, M. J. Palladium-catalyzed highly regioselective mono and double Sonogashira cross-coupling reactions of 5-substituted-1,2,3-triiodobenzene under ambient conditions. *RSC Adv.* **10**, 16366–16376 (2020).
26. Budarin, V., Shuttleworth, P., Clark, J. & Luque, R. Industrial applications of CC coupling reactions. *Curr. Org. Synth.* **7**, 614–627 (2010).
27. Colacot, T. J. The 2010 Nobel Prize in chemistry: Palladium-catalysed cross-coupling. *Platin. Met. Rev.* **55**, 84–90 (2011).
28. Sonogashira, K., Tohda, Y. & Hagihara, N. A convenient synthesis of acetylenes: Catalytic substitutions of acetylenic hydrogen with bromoalkenes, iodoarenes and bromopyridines. *Tetrahedron Lett.* **16**, 4467–4470 (1975).
29. Ferlin, F. *et al.* Biomass waste-derived Pd-PiNe catalyst for the continuous-flow copper-free sonogashira reaction in a CPME-water azeotropic mixture. *ACS Sustain. Chem. Eng.* **9**, 12196–12204 (2021).
30. Tan, E., Quinonero, O., ElenadeOrbe, M. & Echavarren, A. M. Broad-scope Rh-catalyzed inverse-Sonogashira reaction directed by weakly coordinating groups. *ACS Catal.* **8**, 2166–2172 (2018).
31. Mohajer, F., Heravi, M. M., Zadsirjan, V. & Poormohammad, N. Copper-free Sonogashira cross-coupling reactions: An overview. *RSC Adv.* **11**(12), 6885–6925 (2021).
32. Nasseri, M. A., Rezazadeh, Z., Kazemnejadi, M. & Allahresani, A. Magnetic Cu–Schiff base complex with an ionic tail as a recyclable bifunctional catalyst for base/Pd-free Sonogashira coupling reaction. *J. Iran. Chem. Soc.* **16**(12), 2693–2705 (2019).
33. Sobhani, S. & Pakdin-Parizi, Z. Palladium-DABCO complex supported on γ-Fe_2O_3 magnetic nanoparticles: A new catalyst for CC bond formation via Mizoroki-Heck cross-coupling reaction. *Appl. Catal. A Gen.* **479**, 112–120 (2014).
34. Zomorodian, K. *et al.* Modified magnetic nanoparticles by PEG-400-immobilized Ag nanoparticles (Fe_3O_4@PEG–Ag) as a core/shell nanocomposite and evaluation of its antimicrobial activity. *Int. J. Nanomed.* **13**, 3965 (2018).
35. Nasseri, M. A., Allahresani, A. & Esmaeili, A. A. Niobium pentachloride catalyzed one-pot multicomponent condensation reaction of β-naphthol, aryl aldehydes and cyclic 1, 3-dicarbonyl compounds. *Lett. Org. Chem.* **11**, 91–96 (2014).

36. White, B. R., Stackhouse, B. T. & Holcombe, J. A. Magnetic γ-Fe_2O_3 nanoparticles coated with poly-l-cysteine for chelation of As (III), Cu (II), Cd (II), Ni (II), Pb (II) and Zn (II). *J. Hazard. Mater.* **161**, 848–853 (2009).
37. Chang, M., Chang, Y. J., Chao, P. Y. & Yu, Q. Exosome purification based on PEG-coated Fe_3O_4 nanoparticles. *PLoS ONE* **13**, e0199438 (2018).
38. Sardarian, A. R., Eslahi, H. & Esmaeilpour, M. Green, cost-effective and efficient procedure for Heck and Sonogashira coupling reactions using palladium nanoparticles supported on functionalized Fe3O4@SiO2 by polyvinyl alcohol as a highly active, durable and reusable catalyst. *Appl. Organomet. Chem.* **33**, e4856 (2019).
39. Mohammadinezhad, A. & Akhlaghinia, B. Fe3O4@Boehmite-NH2-CoII NPs: An inexpensive and highly efficient heterogeneous magnetic nanocatalyst for the Suzuki-Miyaura and Heck-Mizoroki cross-coupling reactions. *Green Chem.* **19**, 5625–5641 (2017).
40. Murugan, E. & Jebaranjitham, J. N. Dendrimer grafted core–shell Fe_3O_4–polymer magnetic nanocomposites stabilized with AuNPs for enhanced catalytic degradation of Rhodamine B–a kinetic study. *J. Chem. Eng.* **259**, 266–276 (2015).
41. Kühbeck, D., Saidulu, G., Reddy, K. R. & Díaz, D. D. Critical assessment of the efficiency of chitosan biohydrogel beads as recyclable and heterogeneous organocatalyst for C–C bond formation. *Green chem.* **14**, 378–392 (2012).
42. Sardarian, A. R., Kazemnejadi, M. & Esmaeilpour, M. Bis-salophen palladium complex immobilized on Fe_3O_4@SiO_2 nanoparticles as a highly active and durable phosphine-free catalyst for Heck and copper-free Sonogashira coupling reactions. *Dalton Trans.* **48**, 3132–3145 (2019).
43. Jiang, Y. *et al.* A novel nanoscale catalyst system composed of nanosized Pd catalysts immobilized on Fe_3O_4@SiO_2–PAMAM. *Nanotechnology* **19**, 075714 (2008).
44. Baran, N. Y., Baran, T. & Menteş, A. Design of highly robust halloysite nanoclay supported palladium complex as a highly active heterogeneous catalyst for construction of biaryls. *Appl. Clay Sci.* **181**, 105225 (2019).
45. Darezereshki, E. Synthesis of maghemite (γ-Fe_2O_3) nanoparticles by wet chemical method at room temperature. *Mater. Lett.* **64**, 1471–1472 (2010).
46. Sreeja, V. & Joy, P. Microwave–hydrothermal synthesis of γ-Fe_2O_3 nanoparticles and their magnetic properties. *Mater. Res. Bull.* **42**, 1570–1576 (2007).
47. Liu, Y. *et al.* Copper-catalyzed sonogashira reaction in water. *ChemistrySelect* **2**, 11599–11602 (2017).
48. Liori, A. A., Stamatopoulos, I. K., Papastavrou, A. T., Pinaka, A. & Vougioukalakis, G. C. A sustainable, user-friendly protocol for the Pd-free sonogashira coupling reaction. *Eur. J. Org. Chem.* **2018**, 6134–6139 (2018).
49. Song, J. Y. *et al.* Visible-light-assisted cobalt-2-(hydroxyimino)-1-phenylpropan-1-one complex catalyzed Pd/Cu-free Sonogashira-Hagihara cross-coupling reaction. *ChemCatChem* **10**, 758–762 (2018).
50. Hajipour, A. R., Rezaei, F. & Khorsandi, Z. Pd/Cu-free Heck and Sonogashira cross-coupling reaction by Co nanoparticles immobilized on magnetic chitosan as reusable catalyst. *Green Chem.* **19**, 1353–1361 (2017).
51. Li, Y., Feng, X. & Li, Z. Visible-light-initiated Sonogashira coupling reactions over CuO/TiO_2 nanocomposites. *Catal. Sci. Technol.* **9**, 377–383 (2019).
52. Wang, B. *et al.* Photocatalytic Sonogashira reaction over silicon carbide supported Pd–Cu alloy nanoparticles under visible light irradiation. *Catal. Sci. Technol.* **8**, 3357–3362 (2018).
53. Beletskaya, I. P. & Cheprakov, A. V. Copper in cross-coupling reactions: The post-Ullmann chemistry. *Coord. Chem. Rev.* **248**, 2337–2364 (2004).
54. Li, J. H. *et al.* CuI-catalyzed Suzuki–Miyaura and Sonogashira cross-coupling reactions using DABCO as ligand. *Coord. Chem. Rev.* **72**, 2053–2057 (2007).
55. Oka, H., Kitai, K., Suzuki, T. & Obora, Y. N, N-Dimethylformamide-stabilized copper nanoparticles as a catalyst precursor for Sonogashira-Hagihara cross coupling. *RSC Adv.* **7**, 22869–22874 (2017).

Acknowledgements

Authors gratefully acknowledge the financial support by the Research Council of University of Birjand, Birjand, Iran.

Author contributions

S.S., visualization, data curation, analysis, investigation, writing—original draft. M.A.N., supervision, conceptualization, funding acquisition, methodology. A.A., softwares, project administration, Validation. R.S.V., validation, project administration, writing-Review and editing.

Competing interests

The authors declare no competing interests.

Additional information

Supplementary Information The online version contains supplementary material available at https://doi.org/10.1038/s41598-022-22567-5.

Correspondence and requests for materials should be addressed to S.S. or M.A.N.

Reprints and permissions information is available at www.nature.com/reprints.

Publisher's note Springer Nature remains neutral with regard to jurisdictional claims in published maps and institutional affiliations.